

Theory of Si 2*p* core-level shifts at the Si(001)-SiO₂ interface

Alfredo Pasquarello

*Institut Romand de Recherche Numérique en Physique des Matériaux (IRRMA), IN-Ecublens, CH-1015 Lausanne, Switzerland
and AT&T Bell Laboratories, 600 Mountain Avenue, Murray Hill, New Jersey 07974*

Mark S. Hybertsen

AT&T Bell Laboratories, 600 Mountain Avenue, Murray Hill, New Jersey 07974

Roberto Car

*Institut Romand de Recherche Numérique en Physique des Matériaux (IRRMA), IN-Ecublens, CH-1015 Lausanne, Switzerland
and Department of Condensed Matter Physics, University of Geneva, CH-1211 Geneva, Switzerland*

(Received 18 December 1995)

A first-principles investigation of Si 2*p* core-level shifts at the Si(001)-SiO₂ interface is presented. We introduce several relaxed interface models obtained by attaching different crystalline forms of SiO₂ to Si(001). These model structures contain the minimal transition region required to accommodate the three intermediate oxidation states of silicon, in accord with photoemission experiments. The bond density mismatch is fixed by saturating all the bonds, as required by electrical measurements. Calculated core shifts are primarily affected by the number of nearest-neighbor oxygen atoms, showing a linear dependence. This result confirms the traditional interpretation of the photoemission spectra based on a charge-transfer model. Core relaxation plays a significant role accounting for more than 50% of the total shifts. The shifts are found to be essentially insensitive to second and further neighbors in the structure. Structural deformations, such as those implied by the distribution of Si-O bond lengths in *a*-SiO₂, yield distributions of core-level shifts that are too small to account for the observed width of the photoemission peaks. In the oxide, we observe a spatial dependence of the Si⁺⁴ shifts with distance from the interface plane. We relate this behavior to the dielectric discontinuity at the interface and suggest that this effect explains the shift of the Si⁺⁴ with oxide thickness, observed in photoemission experiments.

I. INTRODUCTION

Despite the use of a large variety of experimental techniques,¹⁻³ the combined effect of a few factors, such as the difficulty of accessing a buried interface, the amorphous nature of the SiO₂ component, and the dependence on sample preparation techniques, have so far prevented a complete description of the structural properties at the Si(001)-SiO₂ interface. However, the crucial role of this interface in silicon-based technology, with the present program of device development requiring highly uniform SiO₂ films of less than 100 Å on Si, calls for a better understanding at the microscopic level.

Among the various experimental techniques,¹⁻³ core-level (Si 2*p*) photoelectron spectroscopy (PES) stands out as one of the most successful tools of investigation of the Si(001)-SiO₂ interface.⁴⁻⁶ The binding energy of the Si 2*p* core states is obtained by measuring the kinetic energy of photoexcited electrons. This technique therefore acts as a probe that is mainly sensitive to the local potential, providing a measure of the chemical environment or oxidation state of the silicon atoms. Furthermore, PES has successfully been combined with chemical etching techniques to monitor the Si⁺⁴ as a function of oxide thickness. In this way, a substantial body of experimental results has been obtained, which contains valuable, yet indirect, structural information. In order to extract from these results the underlying structural properties, a reliable theoretical interpretation is needed.

PES experiments at the Si(001)-SiO₂ interface indicate

the presence of a transition region in which three distinct intermediate oxidation states of Si are observed.⁴⁻⁶ These partially oxidized silicon atoms appear in roughly comparable amounts. Their total number has been estimated to be between 0.6 and 1.5 ML.⁶ These results suggest a transition width of 5–8 Å, but a general consensus on this issue has not yet been reached.

The PES results are generally interpreted according to a simple picture in which a charge transfer is assumed from the silicon atoms to the more electronegative oxygen atoms. The various suboxide peaks are then attributed to Si atoms with a different number of nearest-neighbor O atoms. This interpretation has been heavily relied upon, particularly in the construction of structural models. However, this simple picture has been challenged by a recent experiment,⁷ which suggests that second-nearest-neighbor effects might be important. These considerations have led to the proposal of more abrupt interface models that do not contain all the possible oxidation states of Si.⁸ From the theoretical point of view, more involved approaches have attempted to go beyond the charge-transfer model,^{9,10} but until recently a consistent picture had not emerged.

In a preliminary report, we have addressed core-level shifts at the Si(001)-SiO₂ interface using a first-principles approach.¹¹ A prerequisite to this study was the availability of interface models with a realistic local microstructure. Such models had been obtained by attaching tridymite,¹² a crystalline form of SiO₂, to Si(001), and then allowing for full relaxation. Calculation of initial-state core-level shifts at

the interface showed a linear dependence of the shifts on the number of nearest-neighbor oxygen atoms, supporting the charge-transfer model. Making use of auxiliary test molecules, we showed that core-hole relaxation contributed significantly to the shifts. Since also these final-state effects were linear in the number of nearest-neighbor oxygen atoms, the traditional interpretation given to the shifts was confirmed.

Although the principal contributions to the shifts have been recognized, the role of more subtle effects such as the dependence on image charges or on structural deformations have not fully been elucidated. These effects together with dynamical processes affect the widths of the suboxide peaks in the PES spectrum. These widths are found to increase with increasing oxidation state.⁴⁻⁶ A complete understanding of both the sizes of these shifts and of their dependence on oxidation state is still lacking.

In this work, we extend our study of core-level shifts at the Si(001)-SiO₂ interface. The general purpose is to clarify the relationship between the shifts and the underlying microscopic structure. To this end, we construct interface models allowing for a thin transition region. In this way, the distribution of oxidation states can be taken consistent with PES data. The models are derived by attaching a crystalline form of SiO₂, either tridymite or β -cristobalite, to Si(001). Examination of these models allows us to study the sensitivity of the core-level shifts to variations in the local microstructure around the silicon atoms. By complementing this study with the calculation of core-level shifts in test molecules, we give an estimate of the dependence of the shifts on structural deformations. Furthermore, extending our first-principles approach, we calculate core-level shifts, including final-state effects directly at the model interface. This allows us to determine the effect of the dielectric discontinuity across the interface on core-hole relaxation. The results are compared to those obtained with a classical model.

This paper is organized as follows. In Sec. II, the method we used to calculate the Si 2*p* core-level shifts is described. The performance of the technique is then tested on a few small molecules in Sec. III. In Sec. IV, we focus on the effect of structural deformations in test molecules. The central part of this work is given in Sec. V, which is devoted to the Si(001)-SiO₂ interface. After introducing the model interfaces, the Si 2*p* shifts are calculated within the initial-state approximation and including core-hole relaxation. The results are supported by a classical calculation to evaluate the effect of image charges. The paper concludes with a discussion in Sec. VI.

II. CALCULATION OF Si 2*p* CORE-LEVEL SHIFTS

A recent study within the local density approximation (LDA) to density functional theory (DF) has shown that calculated carbon 2*p* core-level shifts in a series of molecules differ by less than 0.5 eV from the corresponding experimental values.¹³ In this work we adopt the same theory to calculate Si 2*p* core-level shifts. In this section, we describe our approach and test its performance on a few atomic configurations.

We calculated core shifts both within the initial-state approximation and including core-hole relaxation effects. In

TABLE I. Pseudopotential parameters defining the Si pseudopotential with a screened 2*p* hole used in this work. The functional form used is given in the text. Energies are given in hartree units.

Si ⁺	<i>l</i> =0	<i>l</i> =1	<i>l</i> =2
α_c	0.9894		
α_l	1.5044	1.1613	1.0367
a_l	10.15053	2.85665	-5.11224
b_l	-5.27605	-1.23602	1.41009

order to describe relatively large systems, we make use of the pseudopotential (PP) approach in which core electrons are not explicitly considered. This difficulty is overcome as follows. Relative initial-state shifts are obtained in first-order perturbation theory.^{9,14} We evaluate the expectation value of the local self-consistent potential on the atomic 2*p* orbital. Final-state effects are included following the procedure of Ref. 15. The core-hole binding energy is the difference in total energy between the ionized (E_+) and the neutral state (E_0). The relative shift in the binding energy is then the difference with respect to the reference configuration:

$$\Delta E_b = [E_+ - E_0] - [E_+^{\text{ref}} - E_0^{\text{ref}}]. \quad (1)$$

This double difference is regrouped to involve only differences in energy calculated for the ground state and for the case with a core hole present. This allows use of the PP approach. Two separate calculations are performed. In a first step the ground state is determined. Then, the PP of a given atom is replaced by another PP, which simulates the presence of a screened 2*p* hole in its core. In this work, we did not consider splitting or spin-orbit hybridization of the 2*p* level induced by the crystal field.^{9,14}

In our calculations we determined the electronic ground state using a conventional norm-conserving PP for silicon.¹⁶ We generated a norm-conserving PP with a 2*p* hole (thus, with a valence charge of $Z_v=5$) with the method of von Barth and Car.¹⁷ The functional form of the semilocal potential is given by

$$V_l(r) = -\frac{Z_v}{r} \text{erf}(\sqrt{\alpha_c} r) + (a_l + b_l r^2) e^{-\alpha_l r^2}, \quad (2)$$

where *l* specifies the angular momentum component. The values of the parameters that we used are given in Table I and were obtained by a fitting procedure.¹⁷ Transferability tests, given in Table II, show that this PP is as accurate as the conventional PP we used for Si.¹⁶

In Table III, we report the result of atomic calculations in which PP and all-electron (AE) Si 2*p* shifts are compared. The AE initial-state shifts correspond to the actual shift of the Si 2*p* core eigenvalue, and the full shift is obtained by considering energy differences between two AE total-energy calculations. The AE entries are thus the exact results for the LDA-DF theory and can be used as a reference. The PP shifts have been obtained as described above. PP full shifts are found to be extremely close to the AE ones over a large range of shifts supporting the validity of our approach. Initial-state AE and PP are less close, indicating the limits of first-order perturbation theory. Better agreement is expected when the size of the shifts is smaller.¹⁴ Table III shows that

TABLE II. Transferability tests on a few excited configurations of the Si pseudopotential (PP) with a screened $2p$ hole. (Ref. 17). All-electron (AE) and PP total energies are given with respect to the ground-state $3s^23p^2$ configuration. Energies are in Rydberg.

Configuration	$\Delta E_{\text{tot}}^{\text{AE}}$	$\Delta E_{\text{tot}}^{\text{PP}}$
s^2p^2	0	0
s^1p^3	0.6036	0.6034
$s^2p^1d^1$	0.7414	0.7406
$s^1p^2d^1$	1.3588	1.3575
s^2p^1	1.3943	1.3932
s^1p^2	2.0354	2.0331

in the isolated Si atom core-hole relaxation contributes about 15% of the full shift. However, this result can vary and depends on the bonding environment, as we will see below.

III. SMALL MOLECULES

In order to estimate the DF-LDA errors in calculating Si $2p$ shifts, we now apply our method to a few molecules, for which the shifts are known experimentally. We considered SiH_4 , $(\text{SiH}_3)_2\text{O}$, SiClH_3 , and SiCl_4 . In the calculations, we took bond lengths of 1.50 and 2.01 Å for the Si–H and Si–Cl bonds, respectively. The experimental geometry with a Si–O bond of 1.63 Å and a Si–O–Si angle of 144° was taken for disiloxane.¹⁸ The calculations were performed using a conventional norm-conserving PP for silicon and chlorine,¹⁶ the Coulomb potential for hydrogen, and an ultra-soft PP for oxygen.¹⁹ The valence wave functions were expanded in a set of plane waves defined by a cutoff energy of 16 Ry. Use of a cutoff of 32 Ry yielded shifts differing by less than a tenth of an eV. In particular, we tested the shift of the $3s^13p^3$ configuration with respect to the $3s^23p^2$ one in the isolated Si atom. Using a cutoff of 16 and 32 Ry we obtained -1.34 and -1.37 eV, respectively. This compares well with the numerically accurate value of -1.41 eV, known from the atomic calculation (see Table III). Exchange and correlation were included using the parametrization of Perdew and Zunger.²⁰ In the case of disiloxane, because of the presence of the oxygen atom, we used a cutoff density of 150 Ry for the augmented electron density.²¹ Energy minimization was performed using the Car-Parrinello method.²²

TABLE III. Comparison of calculated all-electron (AE) and pseudopotential (PP) Si $2p$ core-level shifts for a few excited atomic configurations. Shifts are given with respect to the ground-state configuration $3s^23p^2$. Initial-state shifts and full shifts including core-hole relaxation are given separately. The shifts are in eV.

Configuration	Initial state		Full	
	PP	AE	PP	AE
s^2p^2	0	0	0	0
s^1p^3	-1.31	-1.57	-1.41	-1.39
$s^2p^1d^1$	-4.93	-5.15	-4.24	-4.20
$s^1p^2d^1$	-5.85	-6.39	-5.37	-5.36
s^2p^1	-9.41	-9.52	-11.13	-11.15
s^1p^2	-10.63	-11.03	-12.45	-12.43

TABLE IV. Comparison of calculated Si $2p$ shifts with experiment for a few molecules. The shifts are measured with respect to SiH_4 . Experimental data are from Ref. 25. Shifts are in eV.

	Initial state	Full	Expt.
SiH_4	0	0	0
$(\text{SiH}_3)_2\text{O}$	-0.48	-0.94	-0.53
SiClH_3	-0.85	-0.99	-0.83
SiCl_4	-2.98	-3.44	-3.11

The convergence was accelerated making use of a preconditioned damped molecular-dynamics technique.²³ A detailed description of our method can be found in Ref. 21.

The calculations were performed in a periodically repeated cubic cell of varying size (up to 16 Å). The initial-state shifts were obtained by calculating the expectation value of the local self-consistent potential in Fourier space. The full shifts were obtained by performing a separate calculation as described above in the presence of a negative background, in order to assure charge neutrality. The effect of the use of this background and of periodic boundary conditions were eliminated by extrapolating the results for infinite box size, making use of the correct scaling properties.²⁴ The resulting shifts have been reported in Table IV.

The comparison with experiment²⁵ in Table IV gives an estimate of the accuracy of DF-LDA shifts of the Si $2p$ core level. The sizes of the experimental shifts for these molecules are reproduced within about 0.5 eV. These results suggest that Si $2p$ shifts can be calculated as accurately as C $2p$ shifts.¹³ In general, inclusion of the final-state effects leads to larger core-level shifts for these molecules where the bonds are more ionic than in the reference SiH_4 . We remark that all the calculated shifts systematically overestimate the experimental ones, particularly for the case of disiloxane. The same trend was observed for carbon-based molecules in Ref. 13.

IV. EFFECT OF STRUCTURAL DEFORMATIONS

For the thin oxide film on Si(100), Lu *et al.*⁶ measured full widths at half maximum of 0.41, 0.55, 0.68, 0.70, and 1.13 eV for the Si^0 , Si^{+1} , Si^{+2} , Si^{+3} , and Si^{+4} peaks, respectively, in good agreement with the previous measurements by Himpfel *et al.*⁵ Several effects are expected to contribute to these widths: the core-hole lifetime, dynamical (phonon) broadening, and static disorder. In this section, we investigate the contribution to the shifts arising from structural deformations by using appropriately designed test molecules. This gives insight into the role of static disorder in the observed widths of the peaks.

We chose the molecules in such a way as to reproduce the local structural environment around silicon atoms at the Si(001)- SiO_2 interface. In order to mimic the environment of an atom in the Si substrate, distant from the interface, we considered the tetrahedral molecule $\text{Si}(\text{SiH}_3)_4$. The Si–Si bond length was taken as in bulk Si. To compensate for the slightly higher electronegativity of H atoms,²⁶ we have added a localized Gaussian potential to the H Coulomb potential:

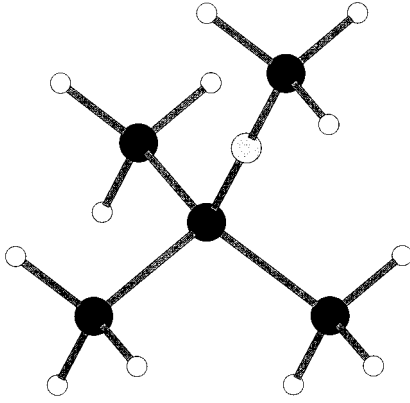


FIG. 1. Ball and stick model of the $\text{SiO}_n(\text{SiH}_3)_4$ test molecule with $n=1$.

$$V_{\text{add}}(r) = A \exp(-r^2/2\sigma^2), \quad (3)$$

where σ was fixed to 1 Bohr radius and A could be chosen in such a way as to depolarize the Si–Si bonds. The Si–Si bonds were monitored by calculating the integrated charge density in two touching spheres centered at one-quarter and three-quarters of the Si–Si bond. Ensuring that these charges were equal minimized the bond polarization. When a cutoff of 16 Ry was used for the wave functions, this gave $A=0.15$ Ry. A comparison with calculations without the potential V_{add} proved that the shifts were negligibly affected, showing differences of about 0.1 eV. We took as a reference the core level of the central Si atom.

In order to study the different oxidation states, we then considered the molecules $\text{SiO}_n(\text{SiH}_3)_4$, where O atoms are inserted in n of the Si–Si bonds (with n varying between 1 and 4). The $n=1$ case is shown in Fig. 1. The Si–O bond length and the Si–O–Si bond angle are fixed to 1.6 Å and 180°, respectively. Application of the same techniques as in the previous section gave the Si 2*p* shifts reported in Table V. The shifts show a linear dependence on the oxidation state n and stress the quantitative importance of core-hole relaxation. Indeed the initial-state approximation severely underestimates the shifts. Such large contributions due to core-hole relaxation are rather unexpected when compared to the case of the isolated Si atom (see Table III), where final-state effects account only for 10–20% of the total shift. The enhancement of the final-state effects can be understood as caused by a reduced valence screening in oxidized Si atoms. The significant contribution due to core-hole relaxation is

TABLE V. Si 2*p* core-level shifts of central Si in the $\text{SiO}_n(\text{SiH}_3)_4$ test molecules (with $n=0,1,\dots,4$), with and without final-state effects. For comparison, we also give the experimental shifts measured at the Si(001)- SiO_2 interface by Lu *et al.* (Ref. 6).

	Initial state	Full	Expt.
$\text{Si}(\text{SiH}_3)_4$	0.00	0.00	0.00
$\text{SiO}(\text{SiH}_3)_4$	−0.52	−1.27	−0.97
$\text{SiO}_2(\text{SiH}_3)_4$	−0.90	−2.40	−1.80
$\text{SiO}_3(\text{SiH}_3)_4$	−1.22	−3.49	−2.60
$\text{SiO}_4(\text{SiH}_3)_4$	−1.66	−4.77	−3.82

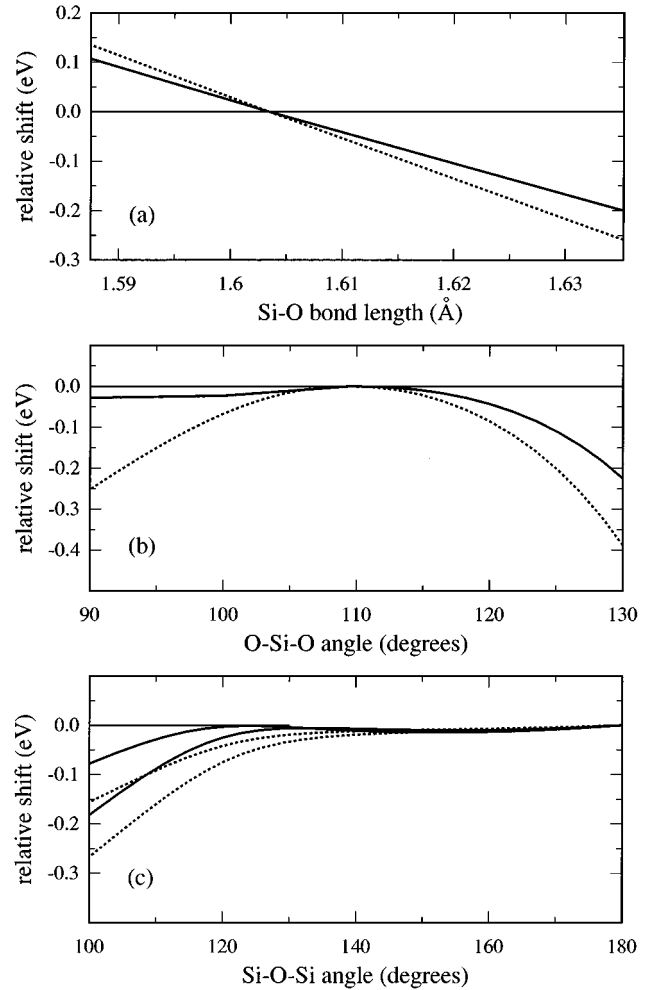


FIG. 2. Initial-state (dotted) and full (solid) shifts of central Si atom in $\text{SiO}_4(\text{SiH}_3)_4$ for distortions of the (a) Si–O bond length, (b) the O–Si–O angles, and (c) Si–O–Si angles (see description in the text). Shifts are given with respect to the shift given in Table V. In (c) the larger relative shifts correspond to a deformation in which a $-\text{SiH}_3$ group is displaced *towards* another one.

confirmed by Auger parameter measurements in SiO_2 , from which a core-hole relaxation energy of 2.0 eV is derived.^{27,28}

We also reproduce in Table V the experimental values for the interface obtained by Lu *et al.*⁶ A direct comparison is complicated by the fact that the effect of long-range relaxation is expected to be poorly reproduced in the test molecules. On one hand the calculated shifts do not reflect the presence of an interface. On the other hand the experimental shifts were measured on an extremely thin film of 5 Å. Nevertheless, the interpretation that attributes the equally spaced suboxide peaks to the presence of silicon atoms with a different number of nearest-neighbor oxygen atoms is strongly supported.^{11,29}

In Fig. 2(a) we give calculated shifts in $\text{SiO}_4(\text{SiH}_3)_4$ for varying Si–O bond lengths. The shifts are found to depend linearly on the bond length in the range considered here. In the calculation, only the distances between the central Si atom and its neighbor oxygen atoms were allowed to vary. The full width at half maximum (FWHM) in the bond-length distribution in amorphous SiO_2 is about 0.08 Å.³⁰ The dependence on bond length in Fig. 2(a) implies a distribution in

core-level shifts of about 0.5 eV, FWHM. Though not negligible, this is insufficient to explain the width observed in PES experiments.^{5,6} Shifts corresponding to other oxidation states also show a linear, but weaker, dependence on the Si–O bond length.

Angular deformations yield substantially smaller shifts. We first considered distortions of the O–Si–O angles. To illustrate their effect on the shifts, we studied deformations in $\text{SiO}_4(\text{SiH}_3)_4$ in which one $-\text{O}^*\text{SiH}_3$ group is kept fixed whereas the other three groups are displaced symmetrically in an ‘‘umbrella’’ fashion. The results obtained for the shifts on the central Si atom are given in Fig. 2(b) as a function of the O–Si–O* angle. Considerations of other types of O–Si–O distortions or of other partial oxidation states of the central Si atom yield similar variations of the shifts. Then we also considered distortions of the Si–O–Si angles. We displaced one $-\text{SiH}_3$ group in a given plane either towards or away from another one. As can be seen from Fig. 2(c), the shifts are rather insensitive to this type of deformation, contrary to an early proposal.³¹ Since the distribution of bond angles of both types in $\alpha\text{-SiO}_2$ has a FWHM of 20° or less,³⁰ the contribution of angular variations to the distribution of core-level shifts is seen to be negligibly small (<0.1 eV). The absence of an important dependence on the Si–O–Si angle is confirmed by a recent PES measurement in which spherosiloxane clusters were deposited on Si(001).³²

We note that for all distortions in Fig. 2 the deviations calculated in the initial-state approximation overestimated those obtained including core-hole relaxation effects.

V. THE Si(001)-SiO₂ INTERFACE

A. Model interfaces

The interface models we considered in this work are all based on interfaces between two periodic structures, Si(001) and a crystalline form of SiO₂. Although the long-range disorder is not taken into account, such models are sufficient for our purpose, since the electronic properties in which we are interested mainly reflect the local microstructure.

We previously introduced two abrupt model interfaces in which tridymite, a crystalline form of SiO₂, had been attached to Si(001).¹¹ The presence of an intralayer of tridymite had first been proposed³³ to account for a metastable interface structure observed by x-ray scattering³⁴ and transmission electron microscopy.³³ Although this interpretation has been controversial,^{35,36} we adopted this model because it was a likely candidate for a structure without unsaturated dangling bonds. This property is suggested by measurements of the interface trap densities, which show that not more than one electronic state in the fundamental gap of Si is found for every 10^4 interface atoms.³⁷ In these interface models, the bond density mismatch was accommodated either by allowing the interface Si atoms to dimerize (model I) or by introducing oxygen bridges (model II).¹¹

In this work we extended the set of models under consideration. In particular, we considered model interfaces that present a transition region containing suboxide. In this way, the distribution of partial oxidation states of silicon atoms could be taken to be consistent with PES experiments.^{5,6} We derived two new model structures from model II using suggestions from Ref. 38. One of the new models [model III,

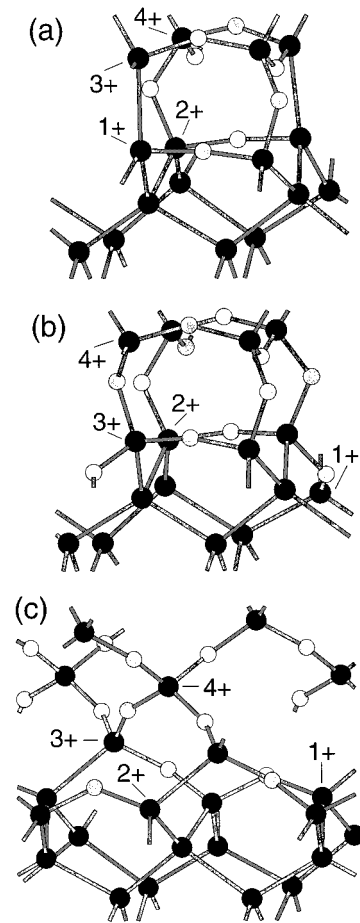


FIG. 3. Ball and stick models showing the relaxed positions of the interface structures introduced in this work: (a) Si–Si bond pointing into the oxide (model III), (b) O in the backbond connecting an interface Si atom to the substrate (model IV), and (c) β -cristobalite with the Ohdomari construction at the interface (model V). The formal Si partial oxidation states are indicated.

Fig. 3(a)] was obtained by eliminating some of the interface oxygen atoms. This gave rise to a Si–Si bond pointing into the oxide. A second new model [model IV, Fig. 3(b)] resulted from the introduction of oxygen atoms in the backbonds connecting silicon interface atoms to the silicon substrate. Models III and IV do not present any unsaturated dangling bonds. In these models the transition region is about 5 Å thick. This choice corresponds to the minimal width required to meet the conditions imposed by PES experiments.

We also added to our set of interface models, a structure [model V, Fig. 3(c)] obtained by attaching β -cristobalite to Si(001).^{39,40} The different crystalline form of SiO₂ used in this model allowed us to discard any specific consequence of the choice of tridymite in the other model structures. In order to fix the bond density mismatch in this model we adopted a construction proposed by Ohdomari *et al.*⁴¹ Model V also meets the conditions required by electrical and PES experiments.

After choosing the topological bond pattern according to the description given above, the atomic coordinates in all of the models were relaxed. We minimized the total energy using the Car-Parrinello method,^{21,22} which provides the

electronic structure as well as the forces that act on the ions. We treated the electronic structure in the same way as described in Sec. III.

Our system contained a 2×2 interface unit of side $L = 7.65 \text{ \AA}$ (based on the theoretical equilibrium lattice constant of Si). The dimension of the cell in the direction orthogonal to the interface was 31.75 \AA , containing 10 layers of Si (13 \AA). In the models in which the oxide was derived from tridymite (models I–IV) we considered 7 monolayers of oxide (9 \AA), whereas we retained 8 monolayers of β -cristobalite in model V (7 \AA). The extremities were saturated with hydrogen atoms. In the minimization process, all the atoms of the oxide as well as the first 6 Si layers were allowed to relax. The Brillouin zone of our simulation cell was sampled using only the Γ point.

At the end of the relaxation process, we found that in all the models the initial topological bond structure had been preserved. The relaxed positions of the atoms close to the interface are shown in Fig. 3 for models III, IV, and V. Analogous figures for models I and II had already been given in Ref. 11. A detailed study of the structural properties in these models, such as bond-length and bond-angle distributions, is given in Refs. 42 and 43. In the oxide, these distributions are found to resemble those of amorphous SiO_2 .³⁰ The bond-length and O-Si-O angle distributions are peaked at 1.62 \AA and at the tetrahedral angle, respectively. The Si-O-Si bond angle distribution is rather broad and reflects the flexibility of this angle. The structural distributions for atoms in the suboxide transition region were found to be broader. We attributed this effect to the presence of a locally strained region at the interface.⁴³ The structural similarities found in the different models support our assumption that the local microstructure is adequately reproduced.

By analyzing the electronic wave functions, we found that in all the models the highest occupied state as well as the lowest unoccupied state are both Si related and do not present any significant weight at the interface. Despite our modest k -point sampling, we were able to conclude that in none of our model structures are there states in the fundamental gap of Si.¹¹

B. Core-level shifts at the interface

We calculated core shifts for the five model structures introduced in the previous section. In this section, the shifts are obtained by adding to the initial-state shifts a correction to account for core-hole relaxation effects. The correction for each oxidation state was taken from the shifts in the corresponding test molecule given in Table V. The shifts calculated within this approximation reproduced within a few tenths of an eV the full shifts obtained for the various distortions in Sec. IV. This approximation is expected to be accurate also at the interface because core-hole relaxation depends primarily on the local structure. We go beyond this approximation in the next section.

In Fig. 4 we collected the Si $2p$ core-level shifts for our five model interface structures. The shifts are plotted as a function of the position of the Si atoms along the direction orthogonal to the interface planes (z axis). We took as a reference value the average shift of atoms in the Si slab

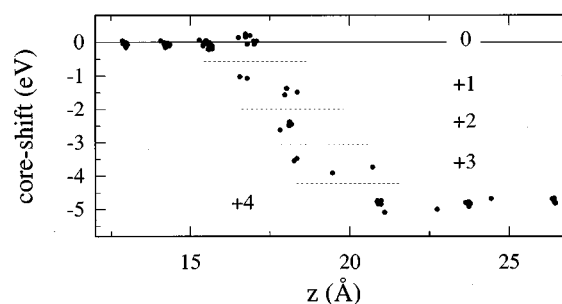


FIG. 4. Composite of the calculated Si $2p$ core-level shifts at the Si(001)- SiO_2 interface along the z direction, orthogonal to the interface plane, for the five models considered in the present work. Core-hole relaxation is included as an additive correction. The different oxidation states of silicon are indicated.

sufficiently distant (sixth to eighth monolayer) from the interface, but far enough from the hydrogen terminated surface.

In the substrate and in the oxide, away from the interface, the shifts do not depend on their position along the z axis, defining the Si^0 and Si^{+4} oxidation states, respectively. In the transition region at the interface, the shifts cluster in three groups, which correspond to intermediate oxidation states of silicon, as indicated in Fig. 3 and in Ref. 11. In order to emphasize the dependence on oxygen coordination, the same shifts are displayed in Fig. 5 as a function of the number of nearest-neighbor oxygen atoms, showing a linear relationship. For comparison we also reported in Fig. 5 experimental values from Ref. 6. The calculated shifts overestimate the PES values by about 20%, but the overall behavior is well reproduced.

The widths in the distribution of the shifts in Fig. 5 reflect the dependence of initial-state shifts on the structural environment. The typical size of these shifts compares well with those obtained for the test molecules in Sec. IV. According to the latter results this type of broadening is expected to be smaller when core-hole relaxation is properly included.

All the $n=4$ shifts fall relatively close to each other in spite of the broad Si-O-Si bond angle distribution in our models. This confirms that the Si $2p$ core-level shift is rather insensitive to the Si-O-Si bond angle. Our results in Fig. 4 show that the $n=4$ shift is rather constant for distances very

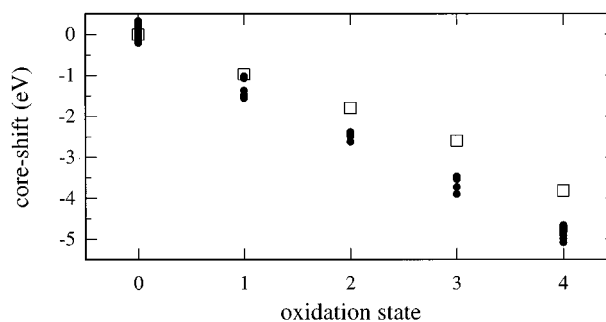


FIG. 5. Si $2p$ core-level shifts at the Si(001)- SiO_2 interface as a function of oxidation state: models (solid circles) and experiment (open squares) from Ref. 6.

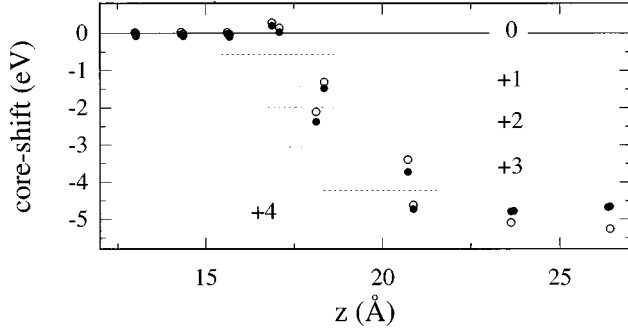


FIG. 6. Si $2p$ core-level shifts at the Si(001)-SiO₂ interface along the z direction, orthogonal to the interface plane, for model III, shown in Fig. 3(a). Shifts that include core-hole relaxation as an additive correction (solid circles) are compared to shifts directly evaluated at the interface (open circles). The different oxidation states of silicon are indicated.

close to the interface. This suggests that the structural properties of the oxide do not undergo any change as a function of distance to the interface. This is indeed confirmed by the structural analysis in Ref. 43, where a local strain field could only be detected in the suboxide region.

C. Core-hole relaxation at the interface

In this section we go beyond the approximation in which the core-hole relaxation is included as an additive correction. We calculated the core shifts directly at the interface by calculating total-energy differences. We used the same procedure described in Sec. III to obtain the full shift. The shift at a given Si site is obtained by replacing the Si PP at that site with the Si PP with a screened core hole and performing a separate electronic minimization. Since this procedure is numerically more costly, we limited our study to the case of model III, which contains all the intermediate oxidation states.

In Fig. 6 we compare the shifts obtained in this way to those given in Fig. 5 for the same structural model. The figure shows that the simple approach used in the previous section to include core-hole relaxation effects closely reproduces the shifts calculated directly at the interface. Two differences appear. First, in the transition region, the shifts evaluated at the interface are smaller, bringing theory closer to experiment. Second, in the oxide, the Si⁺⁴ shifts increase as a function of the distance from the silicon substrate.

In order to check the dependence of these results on technical aspects such as the use of a negative background and the interaction with periodic images, we considered a larger interface unit in the plane of the interface. We doubled the size of our system by taking a supercell with a $\sqrt{8} \times \sqrt{8}$ interface unit of side $L = 10.82 \text{ \AA}$ and with the same size in the z direction (31.75 \AA). The shifts obtained in this way differed by at most 0.1 eV from those reported in Fig. 6.

An increase of the Si⁺⁴ shifts with oxide thickness has also been observed experimentally.^{31,44} The interpretation of this behavior is still controversial. This effect has alternatively been attributed to the presence of an interfacial oxide region with modified structural properties,³¹ to the effect related to the charging of the substrate,^{28,44} or to the role of

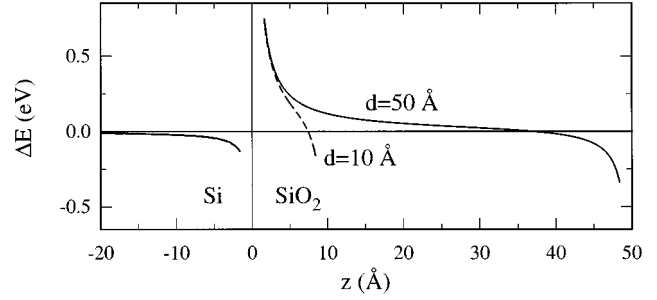


FIG. 7. Correction to the core-hole relaxation energy in the Si-SiO₂-vacuum dielectric system as found with classical electrostatics. The correction is calculated as a function of the position of the excited silicon atom both in the silicon substrate and in the oxide. The solid (dashed) line refers to a 50-Å- (10-Å-) thick oxide.

image charges.⁴⁵ Elucidation of this point is particularly important because it directly yields implications on the width of the transition region, an issue under constant debate. An analysis of the structural properties did not support the presence of a strained oxide region close to the interface,⁴³ as also confirmed by the rather constant $n = 4$ initial-state shifts.

In order to estimate the effect due to the dielectric discontinuity across the interface, we turn to a simple classical model. We consider a system of three dielectrics, separated by abrupt interfaces: a semi-infinite silicon substrate (for $z < 0$ and with ϵ_1), an oxide slab of thickness d ($0 < z < d$, ϵ_2), and the vacuum ($z > d$, ϵ_3). We calculate the correction ΔE to the core-hole relaxation energy due to the presence of the dielectrics. In order to satisfy Maxwell boundary conditions, an infinite series of image charges is required. For an excitation at z in the oxide ($0 < z < d$) we obtain

$$\Delta E = -\frac{1}{2} \frac{e^2}{\epsilon_2} \sum_{n=0}^{\infty} (\eta \xi)^n \left[\frac{\eta}{|2z - 2nd|} + \frac{\xi}{|(2n+1)d - 2z|} + \frac{2\eta\xi}{(2n+2)d} \right], \quad (4)$$

where e is the electronic charge and where

$$\eta = \frac{\epsilon_2 - \epsilon_1}{\epsilon_1 + \epsilon_2} \quad \text{and} \quad \xi = \frac{\epsilon_2 - \epsilon_3}{\epsilon_2 + \epsilon_3}. \quad (5)$$

For an excitation at z in the silicon substrate ($z < 0$)

$$\Delta E = -\frac{1}{2} \frac{e^2}{\epsilon_1} \left[-\frac{\eta}{|2z|} + (1 + \eta)(1 - \eta) \sum_{n=0}^{\infty} \frac{\xi^{n+1} \eta^n}{(2n+2)d - 2z} \right]. \quad (6)$$

The energy ΔE contributes to the shifts as an additive correction provided the sign convention is chosen in which shifts in the oxide are negative with respect to those in the substrate.

In Fig. 7, we displayed these corrections as a function of z coordinate of the excited atom for two different values of the oxide thickness d . We used $\epsilon_1 = 12$, $\epsilon_2 = 2.1$, and $\epsilon_3 = 1$ to describe the Si-SiO₂-vacuum system. The curves in Fig. 7 are interrupted at a distance of 1.6 Å (about a Si-O bond)

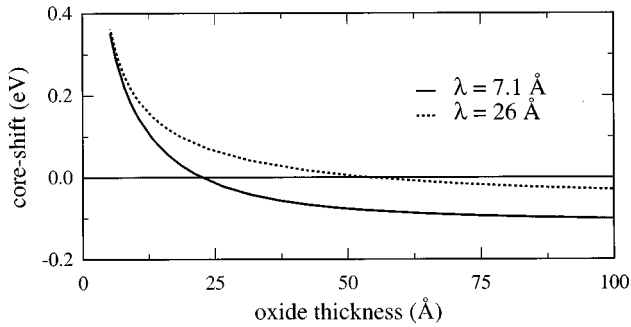


FIG. 8. Correction to the position of the Si^{+4} peak as a function of oxide thickness. The shift is obtained taking into consideration the z dependence of the shifts caused by the dielectric discontinuity across the interface and an exponential weighting function characterized by an escape depth of 7.1 Å (solid) or 26 Å (dotted).

from the interfaces, because of the artificial divergences occurring in classical electrostatics. In the oxide slab, the ΔE decreases with distance to the substrate yielding increasing absolute shifts. The size of the variation of the calculated correction compares well with the dependence of the shifts in Fig. 6. The effect due to image charges is smaller in the substrate, because of the enhanced screening in silicon.

The z dependence of the shifts is expected to affect the position of the Si^{+4} peak in PES spectra. A precise determination of the PES peak position depends on the oxide thickness and on the escape depth. To illustrate this point, we calculated the average shift for varying oxide thickness. We used two ingredients: the z dependence resulting from the electrostatic model and a weighting function characterized by an escape depth λ_{SiO_2} . In order to avoid the unphysical divergences, we did not consider in this calculation contributions coming from regions closer than 1.6 Å to the interfaces. The results from such calculations for two different escape depths are given in Fig. 8. We chose $\lambda_{\text{SiO}_2}=7.1$ Å (Ref. 5) and $\lambda_{\text{SiO}_2}=26$ Å (Ref. 46), which correspond to photon energies of 130 and 1487 eV, respectively. Despite the simplicity of the model, the size of the effect as well as its dependence on oxide thickness compares well with the position of the Si^{+4} peak in PES spectra.^{31,44}

VI. DISCUSSION AND CONCLUSION

Our work shows that the major factor that determines the magnitude of the core-level shifts at the $\text{Si}(001)\text{-SiO}_2$ interface is the number of nearest-neighbor oxygen atoms. As a consequence the traditional interpretation that attributes the suboxide peaks to differently coordinated Si atoms is confirmed.¹¹ We have investigated separately the effect of different contributions to the shifts. A crucial contribution to the calculated shifts was core-hole relaxation. With final-state effects included, the calculated core-level shifts are in good quantitative agreement with experiment. Our study shows that final-state effects are sensitive to the dielectric discontinuity across the interface, giving rise in the oxide to a dependence of the shifts on distance to the interface. We suggest that this effect is a plausible explanation of the shift of the Si^{+4} peak with oxide thickness, observed in PES experiments.

We have investigated the dependence of the shifts on structural properties such as the Si–O bond length. We argued on the basis of the distribution of local structural parameters in $a\text{-SiO}_2$ that the contribution of static disorder to the width for the Si^{+4} PES peak was of order 0.5 eV, substantially smaller than the observed width. The order of magnitude for the lifetime broadening (physically dominated by Auger decay of the core hole) is less than 0.1 eV.⁴⁷ There remains to investigate the role of phonon-induced broadening. A detailed study of this effect, particularly for the interface-related suboxide peaks, is nontrivial and beyond the scope of this paper. However, it is generally known that phonon-induced broadening dominates the width of x-ray photoemission spectroscopy (XPS) peaks in other ionic materials.⁴⁸ Although we are not aware of a detailed study of the temperature dependence of the XPS peaks in $a\text{-SiO}_2$, soft x-ray absorption has been studied recently.⁴⁹ A Gaussian line shape is found with a FWHM of order 0.6 eV. This is consistent with estimates that can be made based on a simple Fröhlich interaction of the core hole with the LO type phonons in the oxide.⁴⁸ Since the interaction of the core-hole exciton studied by soft x-ray absorption is probably screened to some extent, it is plausible that the transitions into continuum states would have an even larger Gaussian width. This is consistent with results for MgO.⁴⁹ Taken together, this suggests that the observed Si^{+4} peak width is consistent with the expected degree of static disorder in $a\text{-SiO}_2$ convolved with a Gaussian line shape attributable to phonon-induced broadening. Details of the peak width for the suboxide contributions depend on the core-hole–phonon coupling near the interface.

The above results lead to the following considerations regarding the microscopic structure at the interface. The main PES features reflect the short-range order around the silicon atoms. The principal structural information conveyed by these experiments is the amount of each distinct formal oxidation state of silicon at the interface. Since the core-level shifts are insensitive to second nearest neighbors, this technique cannot provide a characterization of the bonding topology at the interface. This aspect is confirmed by the small dependence of the shifts on structural deformations.

The experimentally observed shift of the Si^{+4} peak in PES spectra with oxide thickness had been attributed to the existence of a strained region in the oxide.⁴ Although at variance with transmission electron microscopy measurements, this interpretation has led to the assumption that a rather extended (30 Å) interfacial region existed in which the structural properties were different from amorphous SiO_2 . Our study shows that this dependence on oxide thickness can be attributed to the dielectric discontinuity at the interface,⁴⁵ without invoking the presence of any extended strained oxide region³¹ or of any charging of the substrate.⁴⁴ This interpretation is further supported by a structural analysis in which the strain field was found to be localized in the suboxide region.⁴³ Hence, we conclude that PES spectra are consistent with interface models with a minimal transition region (about 5 Å) as studied in this work. This minimal transition is required to accommodate the intermediate oxidation states of silicon.

ACKNOWLEDGMENTS

We are grateful to Dr. A. Dal Corso for help with the generation of the Si PP with the screened $2p$ hole. We ac-

knowledge useful discussions with Dr. L.C. Feldman. Two of us (A.P. and R.C.) acknowledge support from the Swiss National Science Foundation under Grant No. 20-39528.93. The calculations were performed on the NEC-SX3 of the Swiss Center for Scientific Computing (CSCS) in Manno.

- ¹*The Physics of SiO₂ and its Interfaces*, edited by S. Pantelides (Pergamon, New York, 1978).
- ²*The Physics and Chemistry of SiO₂ and the Si-SiO₂ Interface*, edited by C.R. Helms and B.E. Deal (Plenum, New York, 1988).
- ³*The Physics and Chemistry of SiO₂ and the Si-SiO₂ Interface 2*, edited by C.R. Helms and B.E. Deal (Plenum, New York, 1993).
- ⁴P.J. Grunthaner, M.H. Hecht, F.J. Grunthaner, and N.M. Johnson, *J. Appl. Phys.* **61**, 629 (1987).
- ⁵F.J. Himpsel, F.R. McFeely, A. Taleb-Ibrahimi, J.A. Yarmoff, and G. Hollinger, *Phys. Rev. B* **38**, 6084 (1988); in *The Physics and Chemistry of SiO₂ and the Si-SiO₂ Interface* (Ref. 2).
- ⁶Z.H. Lu, M.J. Graham, D.T. Jiang, and K.H. Tan, *Appl. Phys. Lett.* **63**, 2941 (1993).
- ⁷M.M. Banaszak Holl and F.R. McFeely, *Phys. Rev. Lett.* **71**, 2441 (1993).
- ⁸M.M. Banaszak Holl, S. Lee, and F.R. McFeely, *Appl. Phys. Lett.* **85**, 1097 (1994).
- ⁹Y. Miyamoto and A. Oshiyama, *Phys. Rev. B* **44**, 5931 (1991).
- ¹⁰H. Kageshima and M. Tabe, in *Control of Semiconductor Interfaces*, edited by I. Ohdomari, M. Oshima, and A. Hiraki (Elsevier, Amsterdam, 1994).
- ¹¹A. Pasquarello, M.S. Hybertsen, and R. Car, *Phys. Rev. Lett.* **74**, 1024 (1995).
- ¹²R.W.G. Wyckoff, *Crystal Structures*, 2nd ed. (Wiley, New York, 1963), Vol. 1, p. 315.
- ¹³L. Pedocchi, N. Russo, and D.R. Salahub, *Phys. Rev. B* **47**, 12 992 (1993).
- ¹⁴X. Blase, A.J.R. da Silva, X. Zhu, and S.G. Louie, *Phys. Rev. B* **50**, 8102 (1994).
- ¹⁵E. Pehlke and M. Scheffler, *Phys. Rev. Lett.* **71**, 2338 (1993).
- ¹⁶G.B. Bachelet, D.R. Hamann, and M. Schlüter, *Phys. Rev. B* **26**, 4199 (1982).
- ¹⁷For a brief description see A. Dal Corso, S. Baroni, R. Resta, and S. de Gironcoli, *Phys. Rev. B* **47**, 3588 (1993).
- ¹⁸W. Airey, C. Glidewell, A.G. Robiette, and G.M. Sheldrick, *J. Mol. Struct.* **8**, 413 (1971).
- ¹⁹D. Vanderbilt, *Phys. Rev. B* **41**, 7892 (1990).
- ²⁰J.P. Perdew and A. Zunger, *Phys. Rev. B* **23**, 5048 (1981).
- ²¹A. Pasquarello, K. Laasonen, R. Car, C. Lee, and D. Vanderbilt, *Phys. Rev. Lett.* **69**, 1982 (1992); K. Laasonen, A. Pasquarello, R. Car, C. Lee, and D. Vanderbilt, *Phys. Rev. B* **47**, 10 142 (1993).
- ²²R. Car and M. Parrinello, *Phys. Rev. Lett.* **55**, 2471 (1985).
- ²³F. Tassone, F. Mauri, and R. Car, *Phys. Rev. B* **50**, 10 561 (1994).
- ²⁴G. Makov and M.C. Payne, *Phys. Rev. B* **51**, 4014 (1995).
- ²⁵W.B. Perry and W.L. Jolly, *Inorg. Chem.* **13**, 1211 (1974).
- ²⁶A. Redondo, W.A. Goddard III, C.A. Swartz, and T.C. McGill, *J. Vac. Sci. Technol.* **19**, 498 (1981).
- ²⁷S. Kohiki, S. Ozaki, T. Hamada, and K. Taniguchi, *Appl. Surf. Sci.* **28**, 103 (1987).
- ²⁸A. Iqbal, C.W. Bates Jr., and J.W. Allen, *Appl. Phys. Lett.* **47**, 1064 (1985).
- ²⁹More accurate evaluation of core-hole relaxation in the test molecules gave the values reported in Table V, which are slightly larger than those previously reported in Ref. 11.
- ³⁰J. Sarnthein, A. Pasquarello, and R. Car, *Phys. Rev. Lett.* **74**, 4682 (1995); *Phys. Rev. B* **52**, 12 690 (1995).
- ³¹F.J. Grunthaner, P.J. Grunthaner, R.P. Vasquez, B.F. Lewis, J. Maserjian, and A. Madhukar, *Phys. Rev. Lett.* **43**, 1683 (1979).
- ³²S. Lee, S. Maman, M.M. Banaszak Holl, and F.R. McFeely, *J. Am. Chem. Soc.* **116**, 11 819 (1994).
- ³³A. Ourmazd, D.W. Taylor, J.A. Rentschler, and J. Bevk, *Phys. Rev. Lett.* **59**, 213 (1987).
- ³⁴P.H. Fuoss, L.J. Norton, S. Brennan, and A. Fisher-Colbrie, *Phys. Rev. Lett.* **60**, 600 (1988).
- ³⁵H. Akatsu and I. Ohdomari, *Appl. Surf. Sci.* **41/42**, 357 (1989).
- ³⁶T.A. Rabedeau, I.M. Tidswell, P.S. Pershan, J. Bevk, and B.S. Freer, *Appl. Phys. Lett.* **59**, 706 (1991).
- ³⁷S.C. Witczak, J.S. Suehle, and M. Gaitan, *Solid-State Electron.* **35**, 345 (1992).
- ³⁸A.X. Chu and W.B. Fowler, *Phys. Rev. B* **41**, 5061 (1990).
- ³⁹F. Herman and R.V. Kasowski, *J. Vac. Sci. Technol.* **19**, 395 (1981).
- ⁴⁰M. Hane, Y. Miyamoto, and A. Oshiyama, *Phys. Rev. B* **41**, 12 637 (1990).
- ⁴¹I. Ohdomari, H. Akatsu, Y. Yamakoshi, and K. Kishimoto, *J. Non-Cryst. Solids* **89**, 239 (1987); *J. Appl. Phys.* **62**, 3751 (1987).
- ⁴²A. Pasquarello, M.S. Hybertsen, and R. Car, *Appl. Surf. Sci.* (to be published).
- ⁴³A. Pasquarello, M.S. Hybertsen, and R. Car, *Appl. Phys. Lett.* **68**, 625 (1996).
- ⁴⁴Y. Tao, Z.H. Lu, M.J. Graham, and S.P. Tay, *J. Vac. Sci. Technol.* **12**, 2500 (1994).
- ⁴⁵R. Browning, M.A. Sobolewski, and C.R. Helms, in *The Physics and Chemistry of SiO₂ and the Si-SiO₂ Interface* (Ref. 2); *Phys. Rev. B* **38**, 13 407 (1988).
- ⁴⁶M.F. Hochella, Jr. and A.H. Carim, *Surf. Sci. Lett.* **197**, L260 (1988).
- ⁴⁷J.E. Rowe, G.K. Wertheim, and R.T. Tung, *J. Vac. Sci. Technol. A* **7**, 2454 (1989).
- ⁴⁸P.H. Citrin, P. Eisenberger, and D.R. Hamann, *Phys. Rev. Lett.* **33**, 965 (1974).
- ⁴⁹W.L. O'Brien, J. Jia, Q-Y. Dong, T.A. Callcott, J-E. Rubensson, D.L. Mueller, and D.L. Ederer, *Phys. Rev. B* **44**, 1013 (1991); W.L. O'Brien, J. Jia, Q-Y. Dong, T.A. Callcott, D.L. Mueller, and D.L. Ederer, *ibid.* **45**, 3882 (1992).